Table I. AM1 Calculated H-Bonding Interactions for Homo- and Heterodimers of Substituted Benzoic Acids (kcal/mol)

monomer A	monomer B	$-H_{interaction}$
p-nitro	*p*-nitro	6.1
p-amino	*p*-amino	6.1
3,5-dinitro	3,5-dinitro	6.1
3,5-diamino	3,5-diamino	6.3
p-nitro	*p*-amino	6.5
p-nitro	3,5-dinitro	6.7
p-nitro	3,5-diamino	6.6
p-amino	3,5-dinitro	7.2
p-amino	3,5-diamino	6.1
3,5-dinitro	3,5-diamino	7.0

Results and Discussion

In this study we considered all possible dimers between *p*-amino-, *p*-nitro-, *m,m*-diamino-, and *m,m*-dinitrobenzoic acids. The results are indicated in Table I. It is immediately apparent that the heterodimers are generally more stable than the homodimers. Coincidentally, the *m,m*-dinitrobenzoic acid–*p*-aminobenzoic acid dimer (reported by Etter[1]) is the most stable of the group. The implication of the data is that the H bonding within the dimer seems to be of some importance. The accuracy of this prediction was tested by mixing *m,m*-dinitrobenzoic acid with (dimethylamino)benzoic acid to see if a 1:1 crystalline material formed. In this case, H bonding between the nitro and amino groups is precluded by the methylation of the amino groups. Apparently, a stoichiometric mixed solid does form (as evidenced by an unmistakable change in color to red), although the structure has not yet been determined.[7]

In a previous study of hydrogen-bonded dimers of various nitroanilines, we reported that the charge alternation of the individual monomer units was accentuated in each of the monomer units of the dimer.[5] In contrast the local charges on the carbons of the aromatic rings of the various benzoic acids are virtually unchanged upon hydrogen bonding. The foregoing is true irrespective of the substituent groups on the benzoic acids, even when one bears nitro and the other amino groups. One is tempted to note that since there are six π-electrons in the cyclic H-bonding structure formed by a nitro and an amino group, while eight in that formed by two carboxylic acids, aromaticity might be involved. Aromaticity has been discussed with reference to the internal H bonds of the enols of β-dicarbonyl compounds.[8,9] While this concept bears further investigation, the orbitals in neither case seem to support aromaticity. In particular, orbitals that are delocalized over the two H-bonding entities may have nodes between them but not through them.

The H-bonding energies presented here are somewhat lower than those expected from the reported H-bonding energies of gas-phase carboxylic acids. Notably, those reported for formic and acetic acid are roughly twice the calculated values.[10] The AM1 values for the interactions of two formic and acetic acid molecules (6.4 and 6.5 kcal/mol, respectively) are similar to those of the benzoic acids. Previously reported ab initio (STO-3G, DZ, DZ+P) calculations have determined H-bonding energies for the dimers of formic[11,12] and acetic[13] acids close to the accepted experimental gas-phase values.

It seems apparent that the AM1 calculations underestimate the H bonding in the acid dimers. This may be due to a continued slight overestimation of H–H repulsion energies (as in MNDO). One should note that in the carboxylic acid dimers, the two H's from *different* molecules approach each other in the dimer. Perhaps the repulsion between these H's (as calculated by AM1) destabilizes the dimer. This point is illustrated by the fact that AM1 predicts the O–H--O distance in formic acid dimer to be 3.06 Å compared to the experimental value of 2.73 Å.[10] Ab initio optimizations predict 2.54 (STO-3G),[11,12,14] 2.705 (4-31G),[15] 2.700 (DZ),[12] and 2.779 Å (DZ+P).[12] The carboxylic H's are 2.95 Å apart in the AM1 optimized geometry. The longer O–H--O distance in AM1 is consistent with the hypothesis that the differential H--H repulsions are responsible for the low binding energy predicted. For the nitroanilines, and other cases studied, the two H's that are close in the dimer are on the same monomeric unit; therefore, this repulsion does not contribute to the interaction energy. Despite the observation that the AM1 interaction energies are too low for the carboxylic acid dimers, it remains apparent that the relative interaction energies can be useful in predicting the likelihood of 1:1 stoichiometrical cocrystallization of the substituted benzoic acids.

Conclusion

In conclusion, AM1 calculations seem to be a useful tool for estimating the intermolecular interactions that determine whether or not cocrystals will form in preference to crystals of the individual components of a mixture. For the case of substituted benzoic acid, very small energy differences in the H-bonding dimerization energy (~1 kcal/mol) are sufficient to determine which crysta' structure will form.

Acknowledgment. This work was supported in part by a PSC-BHE grant.

(7) Etter, M. C.; Frankenbach, G. M., private communication.
(8) Williams, D. E.; Dumke, W. L.; Rundle, R. E. *Acta Crystallogr.* **1962**, *15*, 627.
(9) Emsley, J. *Struct. Bonding* **1984**, *57*, 147.
(10) Chao, J.; Zwolinski, J. *J. Phy. Chem. Ref. Data* **1978**, *7*, 363.
(11) Del Bene, J. E.; Kochenour, W. L. *J. Am. Chem. Soc.* **1976**, *98*, 2041.
(12) Chang, Y.-T.; Yamaguchi, Y.; Miller, W. H.; Schaefer III, H. F. *J. Am. Chem. Soc.* **1987**, *109*, 7245.
(13) Frurip, D. J.; Curtiss, L. A.; Blander, M. *J. Am. Chem. Soc.* **1980**, *102*, 2610.
(14) Agresti, A.; Bacci, M.; Ranfagni, A. *Chem. Phys. Lett.* **1981**, *79*, 100.
(15) Hayashi, S.; Umemura, J.; Kato, S.; Morokuma, K. *J. Phys. Chem.* **1984**, *88*, 1330.

Chemical Vapor Deposition of Copper from Copper(I) Trimethylphosphine Compounds

M. J. Hampden-Smith,*† T. T. Kodas,*‡
M. Paffett,§ J. D. Farr,§ and H.-K. Shin†

Departments of Chemistry and Chemical Engineering
University of New Mexico
Albuquerque, New Mexico 87131
and CLS-1, Los Alamos National Laboratories
Los Alamos, New Mexico 87545

Received February 2, 1990

Chemical vapor deposition (CVD) of metals from metal organic precursor compounds has been the subject of much

* Authors to whom correspondence should be addressed.
† Department of Chemistry.
‡ Department of Chemical Engineering.

0897-4756/90/2802-0636$02.50/0

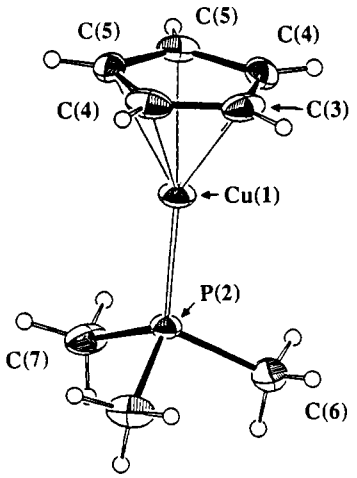

Figure 1. ORTEP plot of η^5-$C_5H_5CuPMe_3$ showing the atom numbering scheme. Important bond distances (Å); Cu–P = 2.113 (1), Cu–Cp(centroid) = 1.867 Å: important angles: P–Cu–Cp(centroid) = 179.5°.

interest in recent years because it is a nondirectional process in which objects with complex shapes or surface topographies may be coated or infiltrated.[1] This is often an advantage over many physical vapor deposition techniques whose line-of-sight nature make coating nonplanar objects difficult. The CVD of metals such as W, Al, Cu, and Au, which are suitable for microelectronic applications, has been studied extensively.[2-6] The physical and chemical properties required of a molecular precursor for CVD include high vapor pressure, low decomposition temperature, and a facile decomposition mechanism allowing clean elimination of the supporting ligands to form a pure deposit. Most studies of metal CVD have employed readily available compounds as molecular precursors, while relatively few studies have utilized species that are tailor-made specifically for this purpose.[7-10] By specifically designing molecular species for CVD, it may be possible to form metal films at lower temperatures, at higher rates, and with higher purities than currently possible.

Of the metals used in microelectronics applications, copper is of great interest as a result of its relatively low resistivity. It is used extensively in packages for electronic chips and is a candidate for the metallization of chips themselves.[11] Precursors for copper CVD have mainly been confined to copper(II) β-diketonates[5,12] because these compounds tend to be air stable and exhibit the highest vapor pressures among compounds that are readily available. However, the films formed from these species often possess oxide or fluoride contamination. For this reason other precursors have been investigated. CVD using copper(I) *tert*-butoxide $[CuO\text{-}t\text{-}Bu]_4$, has produced copper films with carbon contamination below the detection limits of Auger electron spectroscopy (AES) but with oxygen contamination of about 5%.[8a] Cyclopentadienylcopper triethylphosphine, $(\eta^5\text{-}C_5H_5)CuPEt_3$, has been used for laser-induced CVD of copper by photochemically and photothermally induced processes.[13] The purity of spots and lines deposited on polyimide was high, but lines deposited on SiO_2 were contaminated by at least 10% carbon. Possible causes of carbon contamination include low partial pressures of reactive hydrocarbon impurities in the reactor of reactant feed and/or inhomogeneous heating of the substrate. Neither the source of the carbon impurity nor the nature of the volatile byproducts were examined.

As part of our studies of low-temperature CVD of metals,[14] we report here our preliminary findings involving the copper(I) compounds cyclopentadienylcopper trimethylphosphine, $(\eta^5\text{-}C_5H_5)CuPMe_3$, and *tert*-butoxycopper trimethylphosphine, $(t\text{-}BuO)CuPMe_3$.

η^5-$C_5H_5CuPMe_3$, **2**, and t-$BuOCuPMe_3$, **3**, were prepared by the metathesis reactions of eqs 1 and 2, respectively, and were characterized by elemental analysis and IR, NMR, and mass spectroscopies.[15] Both **2** and **3** can be

$$\tfrac{1}{4}[ClCuPMe_3]_4 + Tl(C_5H_5) \rightarrow \underset{\mathbf{1}}{} \qquad \underset{\mathbf{2}}{[(\eta^5\text{-}C_5H_5)CuPMe_3]} + TlCl \quad (1)$$

$$\tfrac{1}{4}[ClCuPMe_3]_4 + K(O\text{-}t\text{-}Bu) \rightarrow \qquad \underset{\mathbf{3}}{[(t\text{-}BuO)CuPMe_3]} + KCl \quad (2)$$

Table I. Summary of the Experimental Conditions Used for Compounds 2 and 3

	reactor temp, °C	precursor temp, °C	film thickness, Å
2, $CpCuPMe_3$			
A	450	40	750
B	330	60	3400
C	260	50	>6000
3, t-$BuOCuPMe_3$			
D	400	60	5250

Table II. Cu Film Purity Determined by Auger Electron Spectroscopy[a]

	purity, atomic concn, %			
sample	Cu	C	O	P
2, $CpCuPMe_3$				
A	84 (1)	16 (1)	*b*	*b*
B	95 (3)	5 (3)	*b*	*b*
C	93 (2)	7 (2)	*b*	*b*
3, t-$BuOCuPMe_3$				
D	90	2	5	3

[a] The average compositions were determined from at least two experiments under each set of conditions. The estimated variance is given in parentheses. [b] The atomic concentration was below the detection limits, ~1%.

§ Los Alamos National Laboratories.

(1) Hess, D. W.; Jensen, K. F. *Microelectronics Processing, Chemical Engineering* Aspects. *Adv. Chem. Ser.* **1989**, *221*.
(2) John, P. In *The Chemicals of the Semiconductor Industry*; Moss, S. J., Ledwith, A., Eds.; Blackie and Son: Glasgow, 1987.
(3) W: Broadbent, E. K.; Stacey, W. T. *Solid State Technol.* **1985**, *28*, 51. Proceedings of the 1988 Workshop on "Tungsten and Other Refractory Materials for VLSI Applications IV" Oct 4–6, Albuquerque, NM; Blewer, R. S.; McConica, C. M., Eds.
(4) Al: Bent, B. E.; Nuzzo, R. G.; Dubois, C. H. *J. Am. Chem. Soc.* **1989**, *111*, 1634 and references therein.
(5) Cu: Houle, F. A.; Jones, C. R.; Baum, T. H.; Pico, C.; Kovac, C. A. *Appl. Phys. Lett.* **1985**, *46*, 204. See also: *Mater. Res. Soc. Symp. Proc. VLSI V* **1990**, 351–373.
(6) Au: Baum, T. H.; Jones, C. R. *Appl. Phys. Lett.* **1985**, *47*, 5381. Baum, T. H.; Jones, C. R. *J. Vac. Sci. Technol., B* **1986**, *48*, 1187. Baum, T. H.; Marinaro, E. E.; Jones, C. R. *Appl. Phys. Lett.* **1986**, *49*, 1213.
(7) Pd/Pt: Gozum, J. E.; Pollina, D.; Jensen, J. A.; Girolami, G. S. *J. Am. Chem. Soc.* **1988**, *110*, 2688.
(8) Al: Gladfelter, W.; Boyd, D. C.; Jensen, K. *Chem. Mater.* **1989**, *1*, 339.
(9) Cu: Jeffries, P. M.; Girolami, G. S. *Chem. Mater.* **1989**, *1*, 8.
(10) Au: Klassen, R. B.; Baum, T. H. *Organometallics* **1989**, *8*, 2477.
(11) Murarka, S.; Peckerar, M. C. *Electronic Materials Science and Technology*; Academic Press: New York, 1989.
(12) Oehr, C.; Suhr, H. *Appl. Phys., A.* **1988**, *45*, 151. Temple, D.; Reisman, A. Technical report number 4, Microelectronic Center of North Carolina, July 28, 1988.
(13) Dupuy, C. G.; Beach, D. B.; Hurst, J. E.; Jasinski, J. M. *Chem. Mater.* **1989**, *1*, 16.
(14) Shin, H.-K.; Hampden-Smith, M. J.; Kodas, T.; Farr, J. D.; Paffett, M. *Proc. Mater. Res. Soc. Symp. J.*, in press.

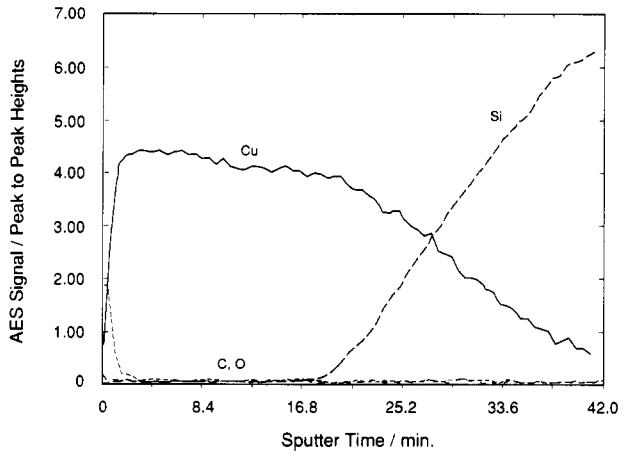

Figure 2. Depth profile of film B.

readily sublimed at 65 °C and 10^{-3} Torr. The structural identity of **2** was confirmed by single-crystal X-ray diffraction[16] as shown in Figure 1. The cyclopentadienyl ring is essentially planar and is bonded in an η^5 fashion to the copper center. The Cu–$C_{centroid}$ (1.867 Å) and Cu–P (2.133 Å) distances of **2** are very similar to those of $(\eta^5\text{-}C_5H_5)$-$CuPPh_3$ (1.864 and 2.135 Å, respectively).[17] The Cu–$C_{centroid}$ distance represents a relatively weak Cu–$(\eta^5\text{-}C_5H_5)$ interaction compared to other late-transition-metal cyclopentadienyl compounds[18] and may account for the relatively facile removal as $(\eta^5\text{-}C_5H_5)^\bullet$ during CVD.

CVD of **2** and **3** onto SiO_2 was carried out in a hot-wall CVD reactor at a pressure of approximately 10^{-3} Torr under dynamic vacuum. The conditions for each experiment are given in Table I. The average film compositions as determined by Auger electron spectroscopy (AES) are presented in Table II.[19] Each CVD experiment was performed at least twice, and the average composition is given together with the variance. Deposition rates were estimated from the film thickness (stylus and AES profilometry) and the deposition time to be in the range 6–100 Å/min. In some cases the SiO_2 substrate was observed at very early times in the sputter depth profile. Scanning electron microscopy (SEM) data show the existence of isolated islands of copper (see the photomicrograph in the supplementary material). We are currently investigating this nucleation problem on SiO_2, but more homogeneous films were obtained when deposition was carried out on SiO_2 substrates that had been coated with 150 Å of Pt. Oxygen and phosphorus contamination levels in all the $(\eta^5\text{-}C_5H_5)CuPMe_3$-derived films were below AES detection limits. Carbon contamination of films deposited on SiO_2 was in the range 2–16% depending on the conditions. The level of carbon contamination varied with the deposition conditions and was lowest at 330 °C with higher levels at both 260 and 450 °C. The depth profile of film B is given in Figure 2. The SEM photograph on film B shown in Figure 3 indicates a polycrystalline granular morphology with a uniform crystallite size of about 2 μm. X-ray powder diffraction data also indicated that the film formed under conditions B is crystalline. Resistivities of films deposited under conditions B on Pt-coated SiO_2 substrates are in the range 10–12 μΩ cm at room temperature. However after annealing the resistivity dropped at 1.8–2.2 μΩ cm, close to the value of bulk copper metal (1.673 μΩ cm at 20 °C). The (*t*-BuO)$CuPMe_3$ (D) precursor produced films with ~10 atom % of C, O, and P contamination under the conditions employed. To better understand the fundamental aspects of copper CVD from these copper(I) precursors, we have studied the byproduct distribution of these reactions.

The condensable reaction byproducts from CVD of both $CpCuPMe_3$ and *t*-BuO$CuPMe_3$ were trapped at −196 °C in a cold trap between the chamber and vacuum pump and analyzed. For **2**, the trapped byproducts were separated into two components, those that distilled at room temperature and 10^{-3} Torr and those that were involatile at this temperature and pressure. Both components were analyzed by multinuclear NMR spectroscopy. The volatile components contained only PMe_3 and cyclopentadiene, by comparison to authentic samples. For conditions B, Table II, cyclopentadiene was present as 7% of the amount of PMe_3, which itself represented 98.7% of the total trapped phosphorus-containing byproducts. The involatile fractions completely dissolved in benzene-d_6 (under dry nitrogen), and NMR spectroscopy revealed the presence of

(15) General synthetic procedures and precautions have been previously described: Lei, D.; Hampden-Smith, M. J.; Duesler, E. N.; Huffman, J. C. *Inorg. Chem.* **1990**, *29*, 795. Synthesis of **2**: $ClCuPMe_3$ (2.00 g, 11.4 mmol) and 3.11 g (11.4 mmol) of TlCp were placed in a 250-mL Schlenk flask, and 100 mL of dry THF was added under dry nitrogen. The yellow solution gradually turned white on stirring at room temperature in the dark for 20 h. The solution was filtered, the white solid was washed with two 10-mL portions of THF, and the filtrates were combined. The volatile components were removed in vacuo to give a white solid, which was sublimed at 65 °C and 10^{-3} Torr to give 1.902 g (9.3 mmol) $CpCuPMe_3$, **2**, yield 82%: ^{1}H NMR (250 MHz, 20 °C, C_6D_6) δ 6.30 (d, 1.5 Hz, 5 H, C_5H_5), 0.56 (d, 7 Hz, 9 H, PMe_3); ^{13}C NMR (62.9 MHz, 20 °C, C_6D_6) δ 95.2 (s, C_5H_5), 16.0 (d, 24 Hz, PMe_3); ^{31}P NMR (101.3 MHz, 20 °C, C_6D_6) δ −39.0 (s). Anal. Calcd for $CuC_8H_{15}P$: C, 47.10, H, 6.90. Found: C, 46.78; H, 6.77. Synthesis of **3**: $ClCuPMe_3$ (2.00 g, 11.4 mmol) and 1.29 g (11.4 mmol) of KO-*t*-Bu were placed in a 250-mL Schlenk flask, and 40 mL of dry THF was added under dry nitrogen at 0 °C. The mixture turned deep yellow and was stirred for 2 h. The volatile components were removed in vacuo; the solid residue was extracted with 40 mL of benzene and then washed with two 5-mL portions. The volatile components were again removed in vacuo, and the solid obtained was sublimed at 80 °C and 10^{-3} Torr to give 1.949 g (9.2 mmol) of pale yellow **3**, *t*-BuO$CuPMe_3$, yield 81%: ^{1}H NMR (250 MHz, 20 °C, C_6D_6) δ 1.56 (s, 9 H, $OCMe_3$), 0.80 (d, 6.4 Hz, 9 H, PMe_3); ^{13}C NMR (62.9 MHz, 20 °C, C_6D_6) δ 67.9 (s, $OCMe_3$), 36.2 (s, $OCMe_3$), 16.2 (d, 21 Hz, PMe_3); ^{31}P NMR (101.256 MHz, 20 °C, C_6D_6) δ −48.4 (s).

(16) Colorless crystals of **2** were grown by slow evaporation of benzene from a saturated solution at 18 °C. The crystal used for the X-ray study was cleaved from a larger crystal 25 × 0.25 × 25 mm), transferred to a goniostat using standard inert atmosphere techniques and cooled to −155 °C for data collection. Crystal data: empirical formula Cu $C_8H_{15}P$, space group $P21/m$, a = 5.689 (2) Å, b = 10.052 (4) Å, c = 8.510 (3) Å, β = 106.19 (2)°, Z = 2. A total of 1134 independent reflections were measured in the range $6 < 2\theta < 45°$ on a Picker four-circle goniostat with a Furnace Monochromator using Mo Kα radiation (λ = 0.710 69 Å) with a continuous θ–2θ scan and scan speed of 8°/min ($2\theta_{max}$ = 45°). Data were reduced to a unique set of intensities and the structure was solved by a combination of direct methods (MULTAN78) and Fourier techniques. All hydrogen atoms were clearly visible in a difference Fourier synthesis phased on non-hydrogen parameters. All hydrogen atoms were refined isotropically, and non-hydrogen atoms anisotropically in the final cycles. No absorbtion correction was performed. A final difference Fourier was featureless, with the largest peak being 0.43 e/Å^3. The final agreement factors were R = 0.0289 and R_w = 0.0317 for 1087 reflections having $F > 2.33\sigma(F)$.

(17) Cotton, F. A.; Takats, J. *J. Am. Chem. Soc.* **1970**, *92*, 2353.

(18) See e.g.: Collman, J. P.; Hegedus, L. S.; Norton, J. R.; Finke, R. G. *Principles and Applications of Organotransition Metal Chemistry*; University Science Books: CA, 1987; pp 165–175, and references therein.

(19) AES depth profiling was accomplished using a 5.0-keV Ar^+ ion beam with a beam current of 0.2 μA rastered over a 250 × 250 μm area. Quantitative estimates of surface impurities are based on sensitivity factors listed in: Davis, L. E.; MacDonald, N. C.; Palmberg, P.; Raich, G. E.; *Handbook of Auger Electron Spectroscopy*; Physical Electronics Industries: Eden Prarie, MN, 1976. Auger electrons were detected with a Physical Electronics cylindrical mirror electron energy analyzer, Model C15-110B. Instrument calibration was performed according to *ASTM Standards on Surface Analysis*; ASTM: Philidelphia, PA, 1986. Film thicknesses were estimated from profilometry measurements made of the sputter craters with a Dektak IIA (Veeco Instruments).

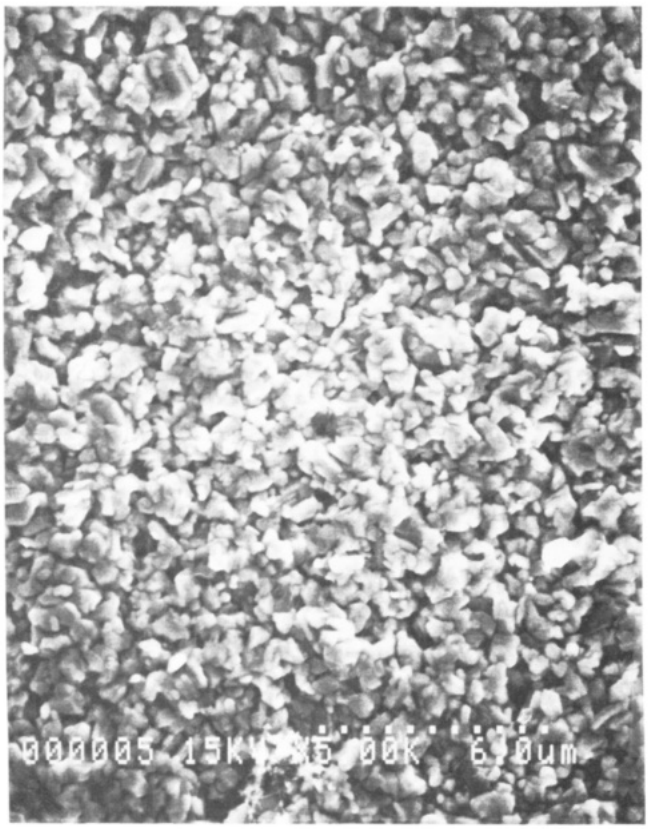

Figure 3. SEM of film B showing a continuous film.

three components derived from the cyclopentadienyl ligand together with a trace of $O{=}PMe_3$ (1.3% of the total phosphorus-containing products).[20] For conditions B, the three components were present in the integrated (^1H NMR) ratio 1:4:2. The species of relative intensity 4 has been identified as 1,5-dihydrofulalene.[21] This mixture is unstable at room temperature and over 4 h completely reacted to produce new unidentified products. Macomber and Rausch[22] observed generation of decamethyl-9,10-dihydrofulvalene during thermal decomposition of η^5-C_5Me_5CuCO in solution at 0 °C. However, 9,10-dihydrofulvalene rearranges unimolecularly at room temperature ($t_{1/2}$ = 53 min at 30 °C) to 1,5-dihydrofulvalene.[21] It therefore seems likely that 9,10-dihydrofulvalene is the kinetic product of combination of cyclopentadienyl radicals, and the majority of rearrangement must have occurred prior to trapping since the isolated byproducts were warmed to room temperature only for 15 min before analysis. The identity of the remaining products is currently under investigation.

Reaction byproducts from CVD of (t-BuO)$CuPMe_3$ were trapped and separated in the same manner as **2**. The volatile components[23] were acetone, isobutene, and *tert*-butyl alcohol[24] and were present in the ratio 1:1:2, respectively, together with PMe_3. The involatile portion consisted only of $O{=}PMe_3$. Acetone, isobutene, and *tert*-butyl alcohol are reasonable decomposition products of t-BuO$^\bullet$ and t-Bu$^\bullet$ radicals and have previously been observed during the CVD of other metal *tert*-butoxide compounds.[25] Of the phosphorus-containing products, $O{=}PMe_3$ was present as 9.4% of the total isolated, the remainder (90.6%) being PMe_3. It is interesting that significantly (7 times) less $O{=}PMe_3$ was observed from the CVD of **2** compared to **3**. It is possible that $O{=}PMe_3$ may have been formed by reaction of PMe_3 with surface oxygen derived from the decomposition of the O-t-Bu ligand.

We note that for **2**, PMe_3 is the major phosphorus-containing byproduct consistent with the efficient cleavage of the Cu–P donor bond, and facile homolysis of the Cu–(η^5-C_5H_5) bond is consistent with the formation of both cyclopentadiene and dihydrofulvalene byproducts. For **3** it appears that the Cu–O bond may not be cleanly cleaved and the presence of a reducing agent (PMe_3) that can scavenge impurities (oxygen) to form volatile and easily removed byproducts ($O{=}PMe_3$) may be an important feature for molecular precursor design.

In summary, these preliminary results indicate that **2** and **3** decompose during CVD according to eqs 3 and 4, respectively. In the case of **2**, there seems to be an optimum range of substrate temperatures (~330 °C) for CVD experiments. Substrate temperatures above and below this range result in significant impurity incorporation. It is likely that the optimum deposition temperature varies as a function of the nature of the CVD precursor and should be taken into account when examining new species. Further studies aimed at determining the roles of gas-phase and surface chemistry during CVD of these and other copper(I) compounds are in progress.

$$\underset{\mathbf{2}}{CpCuPMe_3} \rightarrow Cu + PMe_3 + \text{cyclopentadiene (trace)} + \text{1,5-dihydrofulvalene} + \text{others} \quad (3)$$

$$\underset{\mathbf{3}}{t\text{-BuOCuPMe}_3} \rightarrow Cu + PMe_3 + O{=}PMe_3 + t\text{-BuOH} + \text{acetone} + \text{isobutene} \quad (4)$$

Acknowledgment. We thank Dr. J. C. Huffman of the Molecular Structure Center, Indiana University, for collecting and solving the single-crystal X-ray diffraction data, the NSF Chemical Instrumentation Program for the purchase of a low-field NMR spectrometer, and Spectrum CVD for an equipment donation.

Supplementary Material Available: Tables S1 (bond lengths), S2 (bond angles), S3 (fractional coordinates and thermal parameters), and S4 (anisotropic displacement coefficients), and Figures S1 (space-filling stereoview of **2**), and S2–S3 (NMR data for the volatile reaction byproducts isolated during CVD of **3**), and S4 (SEM of one film deposited under conditions A (Table I) showing islands of copper) (7 pages); Table S5 (listing of observed and calculated structure factors) (3 pages). Ordering information is given on any current masthead page.

(20) Relative ratios of the products of the involatile and volatile fractions were determined by integration of the appropriate ^1H NMR resonances versus the protio impurity in benzene-d_6.

(21) Published NMR data for 1,5-dihydrofulvalene is not very revealing: ^1H NMR ($CDCl_3$) δ 6.5 (m, 2 H), 6.4 (m, 1 H), 3.0 (s, 2 H). Hedaya, E.; McNeil, D. W.; Schissel, P.; McAdoo, D. J. *J. Am. Chem. Soc.* **1968**, *90*, 5824. We observe the following data (benzene-d_6): ^1H NMR 6.44 (m 1 H, H_a), 6.32 (m, 1 H, H_b), 6.13 (m, 1 H, H_c), 2.98 (m, 2 H, H_d). Homonuclear decoupling and 2D COSY experiments confirm a connectivity consistent with 1,5-dihydrofulvalene. ^{13}C NMR δ 133.8 (d), 132.3 (d), 126.9 (d), 41.3 (t). The multiplicities in parentheses are derived from a ^1H-coupled ^{13}C NMR experiment. The quaternary vinyllic carbon has not been unambiguously located yet.

(22) Macomber, D. W.; Rausch, M. D. *J. Am. Chem. Soc.* **1983**, *105*, 5325.

(23) Identified by ^1H, ^{13}C, and ^{13}P NMR and mass spectroscopies.

(24) These results contrast the results obtained from the CVD of [CuO-t-Bu]$_4$ in which t-BuOH was observed as the only reaction byproduct and thought to be derived from t-BuO radical.[9]

(25) Hampden-Smith, M. J.; Smith, D.; Duesler, E. N.; Huffman, J. C. Spring American Chemical Society meeting, Dallas, TX, 1989. See also: Sen, A.; et al. *Inorg. Chem.* **1989**, *28*, 3280.